Received: 2 November 2021 | Revised: 25 January 2022 | Accepted: 2 February 2022

DOI: 10.1111/cas.15296

Cancer Science WILEY

ORIGINAL ARTICLE

Downregulation of miR-26 promotes invasion and metastasis via targeting interleukin-22 in cutaneous T-cell lymphoma

Yuka Matsuda[1] | Sho Ikeda[2] | Fumito Abe[2] | Yuto Takahashi[1] | Akihiro Kitadate[2] | Naoto Takahashi[2] | Hideki Wakui[1] | Hiroyuki Tagawa[2]

[1]Department of Life Science, Graduate School of Engineering Science, Akita University, Akita, Japan

[2]Department of Hematology, Nephrology, and Rheumatology, Akita University Graduate School of Medicine, Akita, Japan

Correspondence
Sho Ikeda, MD, PhD Department of Hematology, Nephrology, and Rheumatology, Akita University Graduate School of Medicine. 1-1-1 Hondo, Akita, Akita 0108543, Japan.
Email: sikeda@med.akita-u.ac.jp

Funding information
This work was supported by JSPS KAKENHI Grant Number 17K09914 (HT) and The Japanese Society of Hematology Research Grant (SI)

Abstract

It has been reported that certain microRNAs (miRNA) are associated with the pathogenesis of lymphoma. We have previously demonstrated that histone deacetylase inhibitors restore tumor-suppressive miRNAs, such as miR-16, miR-29, miR-150, and miR-26, in advanced cutaneous T-cell lymphoma (CTCL). Among these, the function of miR-26 remains unclear. In this study, we aimed to reveal the function of miR-26 in CTCL oncogenesis. First, we confirmed that the miR-26 family was markedly dysregulated in CTCL cell lines and primary samples. *In vivo* analysis using miR-26a-transduced CTCL cells injected into immunodeficient NOG mice demonstrated the significant prolonged survival of the mice, suggesting that the miRNA had a tumor-suppressive function. We performed gene expression assays and identified 12 candidate miR-26 targets, namely *RGS13*, *FAM71F1*, *OAF*, *SNX21*, *CDH2*, *PTPLB*, *IL22*, *DNAJB5*, *CASZ1*, *CACNA1C*, *MYH10*, and *CNR1*. Among these, *IL22* was the most likely candidate target because the IL-22–STAT3–CCL20–CCR6 cascade is associated with tumor invasion and metastasis of advanced CTCL. *In vitro* analysis of IL22 and IL22RA knockdown and miR-26 transduction demonstrated inhibited CTCL cell migration. In particular, IL22 knockdown induced cell apoptosis. Finally, we conducted *in vivo* inoculation analysis of mice injected with shIL22-transfected CTCL cells, and found no tumor invasion or metastasis in the inoculated mice, although the control mice showed multiple tumor invasions and metastases. These results, along with our previous data, demonstrated that miR-26 is a tumor suppressor that is associated with tumor invasion and the metastasis of advanced CTCL by regulating the IL-22–STAT3–CCL20 cascade. Therefore, a IL-22-targeting therapy could be a novel therapeutic strategy for advanced CTCL.

KEYWORDS
CTCL, cutaneous T-cell lymphoma, IL-22, interleukin-22, miR-26

Abbreviations: CTCL, cutaneous T-cell lymphoma; HDAC, histone deacetylase; IL, interleukin; miRNA, microRNA; RT-qPCR, quantitative RT-PCR; Th, T helper.

Yuka Matsuda, Sho Ikeda, and Fumito Abe contributed equally to this work.

1 | INTRODUCTION

Non-Hodgkin lymphoma is classified into various subtypes, including B-cell neoplasms and T/NK-cell neoplasms.[1] Molecular pathogenesis of B-cell lymphomas (i.e., diffuse large B-cell, follicular, and mantle cell lymphomas) have been elucidated by various analyses, including gene expression signatures and genomic structural analyzes.[2-4] Based on these studies, the prognosis of these lymphomas has improved through the development of therapeutic options and novel molecular targeting drugs (e.g., EZH2, Bcl-2, PI3K, and BTK inhibitors).[5,6] However, with the exception of ALK-positive T-cell lymphoma, there have been few therapeutic options in T/NK-cell lymphoma because of insufficient information regarding the responsible target genes/products.[7,8] This may be because conventional detection methods (i.e., genomic structural approaches and gene expression approaches) are limited in detecting targets responsible for T/NK-cell lymphoma. Therefore, we should consider alternative aspects of gene expression aberrations, such as epigenetic alteration in T/NK-cell lymphoma. This is because recent studies have demonstrated that epigenetic gene expression abnormalities may occur more frequently and predominantly in T/NK-cell lymphoma than in B-cell lymphomas.[9,10]

A representative T-cell lymphoma subtype, CTCL, is known to form erythema, patches, plaques, and tumors on the skin with disease progression, leading to multiorgan invasion and poor prognosis.[11,12] Different treatment strategies have been used for early-stage and advanced CTCL.[13,14] Early-stage CTCL is treated with skin-direct therapies (such as phototherapy and topical steroids), while advanced stages are treated with multidrug chemotherapy and/or molecular targeted therapy. In addition to molecular targeted therapies, such as brentuximab vedotin (CD30 antibody) and mogamulizumab (CCR4 antibody), histone deacetylase (HDAC) inhibitors, such as vorinostat and romidepsin, are being used in clinical practice to restore the expression of epigenetically repressed tumor-suppressive genes.[13,14] Notably, epigenetically repressed genes often include tumor-suppressive coding/non-coding genes.[15]

One type of non-coding RNA, microRNA (miRNA), plays crucial roles in cell survival and metabolism.[16] It contributes to gene expression regulation via degradation and translational repression of target messenger RNAs that have specific seed sequences in their 3′ untranslated region (UTR).[16] It has been well documented that, if miRNA is aberrantly expressed, the aberration can induce tumorigenesis via translational repression of target genes and/or their product.[17] We have shown that genomic structural aberration and epigenetic alteration of tumor-suppressive miRNA may occur in various lymphoma subtypes,[18-22] and that the epigenetic alteration occurs predominantly and plays important roles during CTCL development. We found that four miRNA families (miR-15/16, miR-26ab, miR-29abc, and miR-150) were frequently downregulated in advanced CTCL and that these tumor-suppressive miRNA were repressed by HDAC.[21] Among these, we reported that miR-150 downregulation contributed to the multiorgan invasion and metastasis of advanced CTCL by upregulating the expression of its target chemokine receptor CCR6,[18] and that miR-16 induced apoptosis or senescence by targeting BMI-1 in CTCL.[19] Moreover, Kohnken et al.[23] recently reported that miR-29b suppressed oncogenic interleukin (IL)-15 and Notch1 signaling by targeting the transcription factor BRD4 in advanced CTCL. These reports have provided scientific evidence that the restoration of tumor-suppressive miRNA may be a novel potential therapeutic approach for CTCL. However, among the four above-mentioned miRNAs, the significance of miR-26 in CTCL oncogenesis remains unknown. Therefore, we aimed in this study to elucidate the role of miR-26 in CTCL.

2 | MATERIALS AND METHODS

2.1 | Primary samples

This study included six cases of primary CTCL from the Akita University Hospital (Akita, Japan). This study was conducted with written informed consent from the study participants and the approval of the Institutional Review Boards, in accordance with the Declaration of Helsinki, before specimen collection. CD4-positive T cells were collected from healthy donors using magnet beads and autoMACS reagents (Miltenyi Biotec., Bergisch Gladbach, Germany).

2.2 | Cell lines and culture

MyLa was purchased from the European Collection of Cell Cultures. HH, HuT 78, and MJ were purchased from the American Type Culture Collection. These cell lines were cultured in Arteimis-1 medium purchased from Nihon Techno Service (Ibaraki, Japan) with 2% inactivated human serum added. 293FT cells were cultured in DMEM containing 5% inactivated fetal calf serum. Cell counts were conducted using a TC20 Automated Cell Counter (Bio-Rad, Hercules, CA, USA).

2.3 | Microarray

We analyzed miRNA or gene expression using the G2600A SureScan Microarray Scanner System (Agilent, Santa Clara, CA, USA). Experimental protocols were in accordance with Agilent Protocol Ver. 6.7. Data were analyzed using GeneSpring software (Agilent), and uploaded to GSE81190 and GSE180472 in the Gene Expression Omnibus.

2.4 | Transient or stable siRNA or vector transfection

We purchased the following Silencer Select siRNAs from Thermo Fisher Scientific (Waltham, MA, USA): siIL22 #1 (s27046), siIL22 #2 (s27048), siMYC #1 (s9129), and siMYC #2 (s9130). Two siIL22RA

sequences were synthesized as custom-made and purchased from Nippon Gene Material (Toyama, Japan). Information on the siRNA sequences is presented in Table S1. siRNA transfection was performed using Nucleofector II and the Cell Line Nucleofector Kit V (VCA-1003; Lonza, Basel, Germany) in accordance with the manufacturer's protocol. The programs used were as follows: A-023 for CTCL cell lines and Q-001 for 293FT. The method for stable transfection of miRNA-expressing CTCL cells has been previously described.[18]

2.5 | Stable knockdown constructs and lentivirus infection

The IL22 Human shRNA Plasmid Kit (TL303948), including the control plasmid, was purchased from OriGene (Rockville, MD, USA). Information on the shRNA sequences is presented in Table S1. Together with 9.0 μg of the ViraPower Packaging mix (Thermo Fisher Scientific), 3.0 μg of vectors were transfected using Lipofectamine 3000 (Thermo Fisher Scientific) into 293FT cells. After overnight culture, the medium was exchanged to remove transfection reagents. Viral supernatants were harvested at 48 h after transfection. Then, 1×10^6 MyLa cells were prepared with the changed medium and virus-containing medium was added. After 3 days of culture, cells were sorted for GFP expression using a FACSAria III instrument (BD Biosciences, San Jose, CA, USA).

2.6 | Xenograft mouse model

MyLa cells were subcutaneously injected into the right or left side of the body of 6–8-week-old female NOD/Shi-scid IL-2γnul (NOG) mice (Central Institute for Experimental Animals, Kawasaki, Japan). The protocols for animal experimentation described in this paper were approved by the Animal Committee of Akita University.

2.7 | Quantitative RT-PCR (RT-qPCR) analysis

TaqMan probes for GAPDH (Hs02758991_g1), IL22 (Hs00220924_m1), U47 (001223), miR-26a (000405), and miR-26b (000407) were purchased from Applied Biosystems (Foster City, CA, USA). RT-qPCR was performed using a Light Cycler 96 PCR system (Roche, Basel, Switzerland).

2.8 | Northern blot analysis

For northern blot analysis of mature microRNAs, 1 μg of RNA was separated on a 15% denaturing polyacrylamide gel. The control probe sequence is as follows: 5S, TTAGCTTCCGAGATCAGACGA. ^{32}P labeling was used.

2.9 | Dual luciferase assay

We purchased an miTarget miRNA 3′UTR Target Clone (CmiT000001-MT05) as the control vector and a vector containing the IL22 3′UTR (HmiT103252-MT05) from GeneCopoeia (Rockville, MD, USA). We transduced 0.5 μg of these vectors and 1.0 μg of miRNA into 293FT using Amaxa Nucleofector. Next, we exchanged the medium after 24 h. After 48 h, the supernatants were collected. Fluorescence measurements were conducted using an Infinite M200 microplate reader (Tecan, Männedorf, Switzerland), and fluorescence labeling was conducted using the Select-Pair Dual Luminescence Assay Kit (LF031) purchased from GeneCopoeia and in accordance with the manufacturer's protocol.

2.10 | ELISA assay

We purchased Quantikine ELISA Human IL-22 (D2200) from R&D Systems (Minneapolis, MN, USA). The experiments were performed in accordance with the manufacturer's protocol.

2.11 | Western blot analysis

We used a PowerPac Basic power supply, and the Mini-PROTEAN Tetra System and TransBlot Turbo (Bio-Rad) electrophoresis system for western blot analysis in accordance with the manufacturer's protocol. IL-22 antibody (ab124740) was purchased from Abcam (Cambridge, UK). Tubulin (MS-581-P0) was purchased from NeoMarkers (Fremont, CA, USA).

2.12 | Cell migration assay

An *in vitro* cell migration assay was performed using the CytoSelect 96-Well Cell Migration Assay kit 5 μm (CBA-105) from Cell Biolabs (San Diego, CA, USA). First, we transduced miR-26a, miR-26b, siIL22, or siIL22RA into MyLa or HH cells. The medium was exchanged with or without 50 ng/ml IL-22 at 24 h and 48 h. Cells (5×10^5) were transferred to 100 μl of medium without human serum and with or without 50 ng/ml IL-22 in the upper chamber through a coated basement membrane containing 2% human serum and with or without 50 ng/ml IL-22 in the lower chamber. The cells were incubated for 24 h. Migrating cells were counted using a TC20 Automated Cell Counter (Bio-Rad). The protocol is described in Figure 4(A).

2.13 | Cell cycle analyses

The cells were suspended in a mixture containing 0.2 ml of 0.9% NaCl and 3 ml of 70% EtOH, after which the nuclei were stained with propidium iodide (PI) (Sigma-Aldrich, St. Louis, MO, USA). Cellular

DNA content was measured using a FACS Lyric flow cytometry system (BD Biosciences).

2.14 | Reagents

Panovinostat (S1030) was purchased from Selleck (Houston, TX, USA). Vorinostat (A10979) was purchased from AdooQ Bioscience (Irvine, CA, USA). JQ1 (ab141498) was purchased from Abcam. Recombinant human IL-22 (#8931SC) was purchased from Cell Signaling Technology (Danvers, MA, USA).

2.15 | Statistical analysis

Data were analyzed using Student *t*-test or log-rank test (Figure 2C). Bars represent the mean ± 95% confidence interval (CI) of three independent experiments. Asterisks (*) indicate statistical significance: *$0.01 \le p < 0.05$; **$0.001 \le p < 0.01$; ***$p < 0.001$; NS, not significant.

3 | RESULTS

3.1 | miR-26 is downregulated in advanced CTCL via HDAC but not MYC

We previously performed a comprehensive miRNA expression analysis of CTCL cell lines, including MyLa and HH, which were subjected to HDAC inhibitors.[21] We performed a clustering analysis of the data and found that miR-26a is one of the miRNAs whose expression was upregulated by HDAC inhibitors (Figure 1A). To confirm the microarray results, we performed RT-qPCR. As expected, the HDAC inhibitors vorinostat (SAHA) and panobinostat (LBH-589) significantly upregulated miR-26 expression in MyLa (miR-26a) and HH (miR-26a/26b) (Figure 1B). We then performed semi-quantitative analysis (northern blot analysis) of miR-26 in primary samples and cell lines, and found diminished miR-26 expression (Figure 1C). We performed quantitative analysis (RT-qPCR) of miR-26 and found that the extent of downregulation was greater for miR-26a than for miR-26b (Figure 1D). It is known that: (1) miR-26 is downregulated by MYC,[24] and (2) activation of MYC increases during CTCL disease progression.[25] Therefore, we examined the relationship between MYC and miR-26 expression. For this purpose, we transiently transfected CTCL cell lines (MyLa and HuT 78) with siRNAs of MYC. The knockdown efficiency was found to be >50% using RT-qPCR (Figure 1E). Although knockdown of MYC caused a significant upregulation of miR-26 in MyLa and HuT 78, the effect was small (Figure 1E). miR-26 expression recovery was considerably low and unexpected. This may be because the siRNA-induced transient knockdown was immediately inhibited due to a certain feedback mechanism. We investigated MYC inhibition using the BRD4 inhibitor, JQ1. Although JQ1 dramatically reduced MYC expression in a concentration-dependent manner, there was only a slight effect on miR-26a expression restoration, and no effect on miR-26b expression (Figure 1F). These results suggested that miR-26 downregulation was induced by HDAC activation. Moreover, the restoration effect of the HDAC inhibitor was greater than that of the BRD4 inhibitor in advanced CTCL.

3.2 | miR-26 prolongs the survival of CTCL xenografted immunodeficient mice

miR-26 has been shown to be a tumor-suppressive miRNA that was downregulated in numerous cancer types.[26] To examine its potential as a tumor suppressor in CTCL oncogenesis, we conducted an *in vivo* transplantation experiment. First, we established a stable transfectant of miR-26a-expressing MyLa cells. We introduced a control vector and miR-26a expression vector into a CTCL cell line, MyLa, using a lentivirus transfection system, and sorted each with GFP to establish cell lines that stably expressed only GFP (empty; control) or GFP-miR-26a. We examined the expression of miR-26a and miR-26b by northern blot analysis and RT-qPCR, and found a specific restoration of miR-26a expression (Figure 2A,B). In this experiment, we used a well established xenografted mouse model of CTCL, which causes death during days 30–50 through multiple-organ metastasis.[18] We subcutaneously injected GFP-empty MyLa (control, $n = 10$) or GFP-miR-26a MyLa ($n = 10$) cell lines (2×10^5 each) into immunodeficient NOG mice and observed their survival. We found that mice inoculated with GFP-miR-26a MyLa had a significantly prolonged survival time compared with the control group (Figure 2C). This result indicated that miR-26 acts as a tumor suppressor by regulating undetermined targets, at least in advanced CTCL.

3.3 | miR-26 inhibits *IL22*/IL-22 expression and cell invasion in CTCL cells

To identify miR-26-regulated genes in CTCL, we performed a comprehensive gene expression analysis using a cDNA microarray. We found that the expression of 127 genes was reduced by up to one-third in GFP-miR-26a MyLa compared with GFP-empty MyLa (Table S2). Interestingly, Kyoto Encyclopedia of Genes and Genomes (KEGG) pathway analysis of the 127 genes revealed that the Jak–STAT pathway (including *IL22*, *SOCS3*, and *CSF2*/GM-CSF) showed the most significant alteration, and the chemokine signaling pathway (including *CCL17*) was also significantly altered (Figure 3A, left panel). We then performed *in silico* prediction analysis to detect candidate targets of miR-26 against these 127 genes using the TargetScan and microRNA.org programs. Twelve genes, namely *RGS13*, *FAM71F1*, *OAF*, *SNX21*, *CDH2*, *PTPLB*, *IL22*, *DNAJB5*, *CASZ1*, *CACNA1C*, *MYH10*, and *CNR1* were identified (Table 1 and Figure 3A, right panel). Among these, we focused on *IL22* as a direct target of miR-26. This is because we had previously demonstrated that: (1) the IL-22–STAT3 cascade was involved in CTCL tumorigenesis,[18,20] and (2) there were

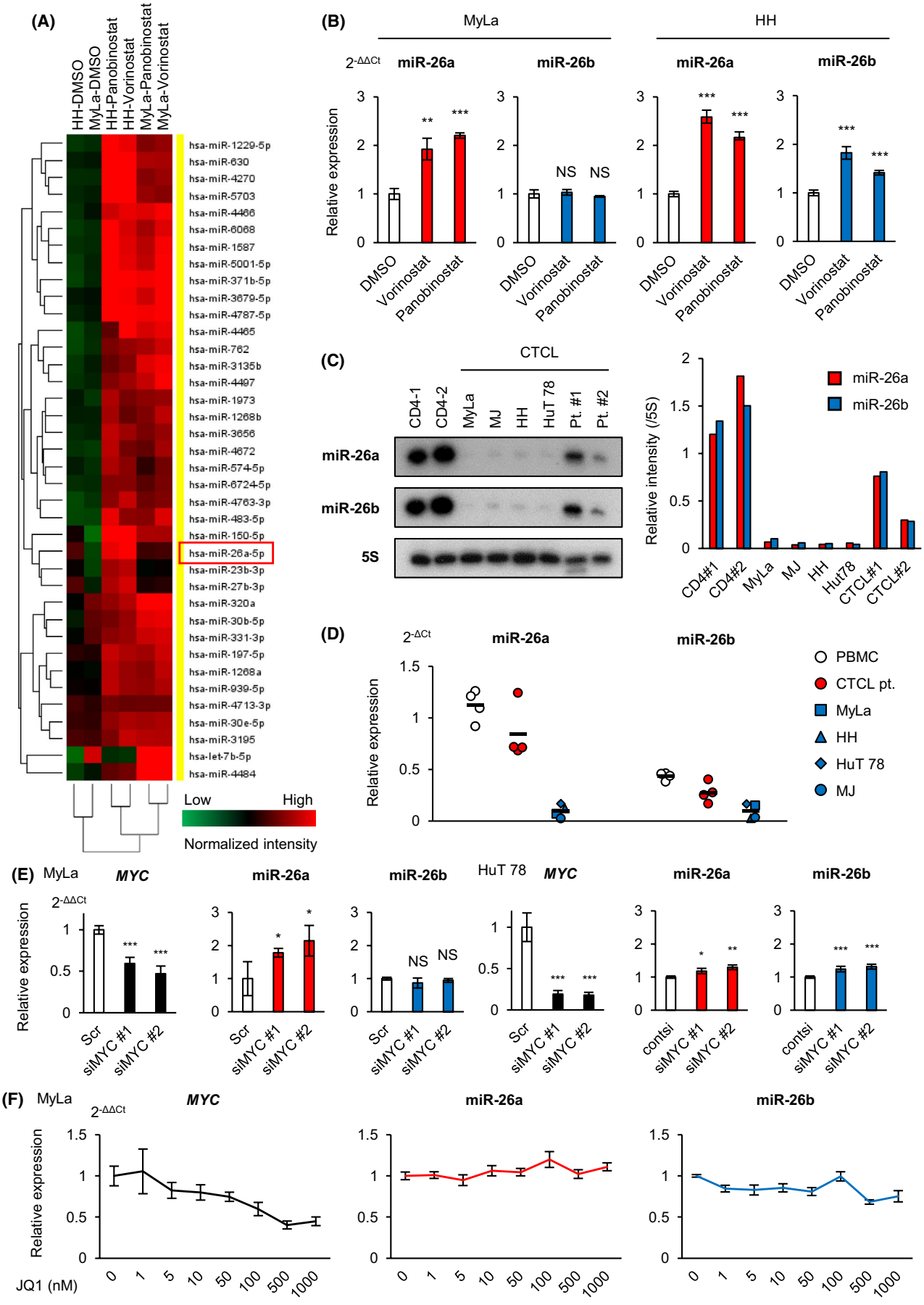

FIGURE 1 miR-26 suppression via histone deacetylase in CTCL cells. (A) Heat map of microRNA expression in MyLa and HH treated with panobinostat (80 nM), vorinostat (4 μM), or dimethyl sulfoxide (DMSO) as the control for 24 h. (B) RT-qPCR analysis of miR-26a/26b in MyLa or HH treated with panobinostat (80 nM), vorinostat (4 μM), or DMSO as the control for 24 h. (C) (Left) Northern blot analysis of miR-26a/26b expression in normal $CD4^+$ T cells, CTCL cell lines (MyLa, MJ, HH, and HuT 78), and primary samples of CTCL (pt. #1 and #2). (Right) Fold changes in miR-26a/26b were determined by densitometry and are shown after normalization to the level of 5S rRNA. (D) RT-qPCR analysis of miRNA-26a/26b in peripheral blood mononuclear cells (PBMC; $n = 4$), primary samples of CTCL ($n = 4$), and indicated CTCL cell lines. (E) RT-qPCR analysis of *MYC*, miR-26a, and miR-26b in MyLa and HuT 78 transduced with siMYC #1, siMYC #2, and scrambled control (Scr) for 24 h. (F) RT-qPCR analysis of *MYC*, miR-26a, and miR-26b for MyLa with the BRD4 inhibitor JQ1 at indicated concentrations for 24 h. Asterisks indicate statistical significance: *$0.01 \le p < 0.05$; **$0.001 \le p < 0.01$; ***$p < 0.001$; NS, not significant. Student *t*-test was used to test for significance. Bars represent the mean ±95% confidence interval of the three replicates

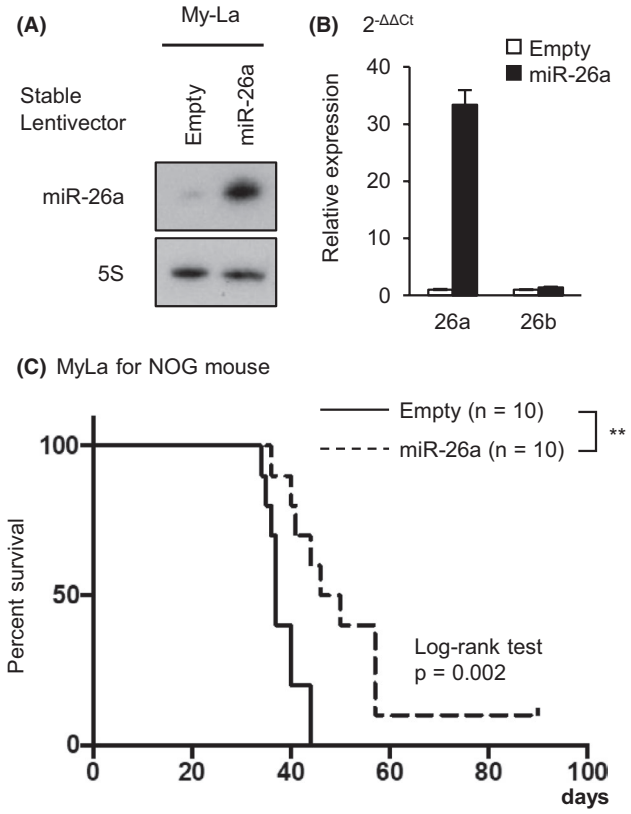

FIGURE 2 miR-26a prolonged survival time in CTCL model mouse. (A) Northern blot analysis of miR-26a in MyLa transduced with GFP-empty vector (control) or GFP-miR-26a vector. (B) RT-qPCR analysis of miR-26a/26b in MyLa transduced with GFP-empty vector (control) or GFP-miR-26a vector. Bars represent the mean ± 95% confidence interval of the three replicates. (C) Survival curves for NOG mouse independently inoculated with MyLa cells transduced with control vector (empty) or miR-26a expressing vector; $n = 10$ each. X-axis: days from inoculation (day 0); Y-axis: survival rate. Asterisks indicate statistical significance: **$0.001 \le p < 0.01$. Log-rank test was used to test for significance

high IL-22 expression levels in the serum and skin lesions of CTCL patients.[18,27,28] miR-26 was likely to bind to the seed sequence of the 3′UTR of *IL22* (Figure 3B), therefore, we conducted a dual luciferase assay and found that miR-26 could directly bind to the 3′UTR of *IL22* and suppress its expression (Figure S1A–D). We further examined the expression of *IL22* and IL-22 in MyLa and HH stably expressing GFP-miR-26a using RT-qPCR and ELISA, respectively, and found that the expression levels of both the mRNA and its product were significantly lower than in controls (Figure 3C). Moreover, we transiently transfected miR-26a and/or miR-26b into MyLa (Figure S2A). Transduction of both miR-26a and miR-26b in MyLa caused a significant decrease in the mRNA and protein expression levels of *IL22*/IL-22, respectively (Figure 3D). However, simultaneous introduction of miR-26a and miR-26b did not show any additive or synergistic effects. These results indicated that miR-26 plays a tumor-suppressive role by suppressing IL-22, which affects the Jak–STAT pathway and chemotaxis mechanisms, in at least in some advanced CTCL cases.

3.4 | Transduction of miR-26 and knockdown of IL22 or IL22RA inhibit CTCL cell migration capability

To determine whether the miR-26–IL-22 axis is involved in chemotaxis and cell migration, we confirmed that miR-26 is effectively transfected into the CTCL cell lines, MyLa and HH (Figure S2A). First, we determined the cell proliferation of these cells and found no significant difference in proliferation rate between control and miR-26-transfected MyLa and HH for 96 h (Figure S2B). Next, we performed a migration assay on CTCL cells. For this, we counted migrated CTCL cells by washing the cells every 24 h and assessing them with or without the addition of external IL-22 (Figure 4A). We found that either miR-26a or miR-26b induced a significant decrease in cell migration, and that the external addition of IL-22 restored its migration capability (Figure 4B). We examined the effects of IL22 and IL22RA knockdown on MyLa. The knockdown efficiency of IL22 was >50% (Figure S2C). Knockdown efficiency of IL22RA was ~60%–80%.[20] We found that knockdown of either IL22 or IL22RA reduced cell migration, and that external addition of IL-22 restored its migration capability (Figure 4C). These results strongly suggested that the miR-26–IL-22 axis is involved in the migration of certain CTCL cells.

3.5 | IL22 knockdown induces prolonged survival of CTCL model mouse

Based on these results, we conducted *in vivo* transplantation in immunodeficient mice to determine the direct role of IL-22 in the invasion and metastasis of CTCL. For this, we established stable IL22-knockdown MyLa using four GFP-shRNA-expressing vectors (named shIL22 #A–D). We found a significant reduction of ~60% mRNA expression in both shIL22 #C and shIL22 #D (Figure 5A).

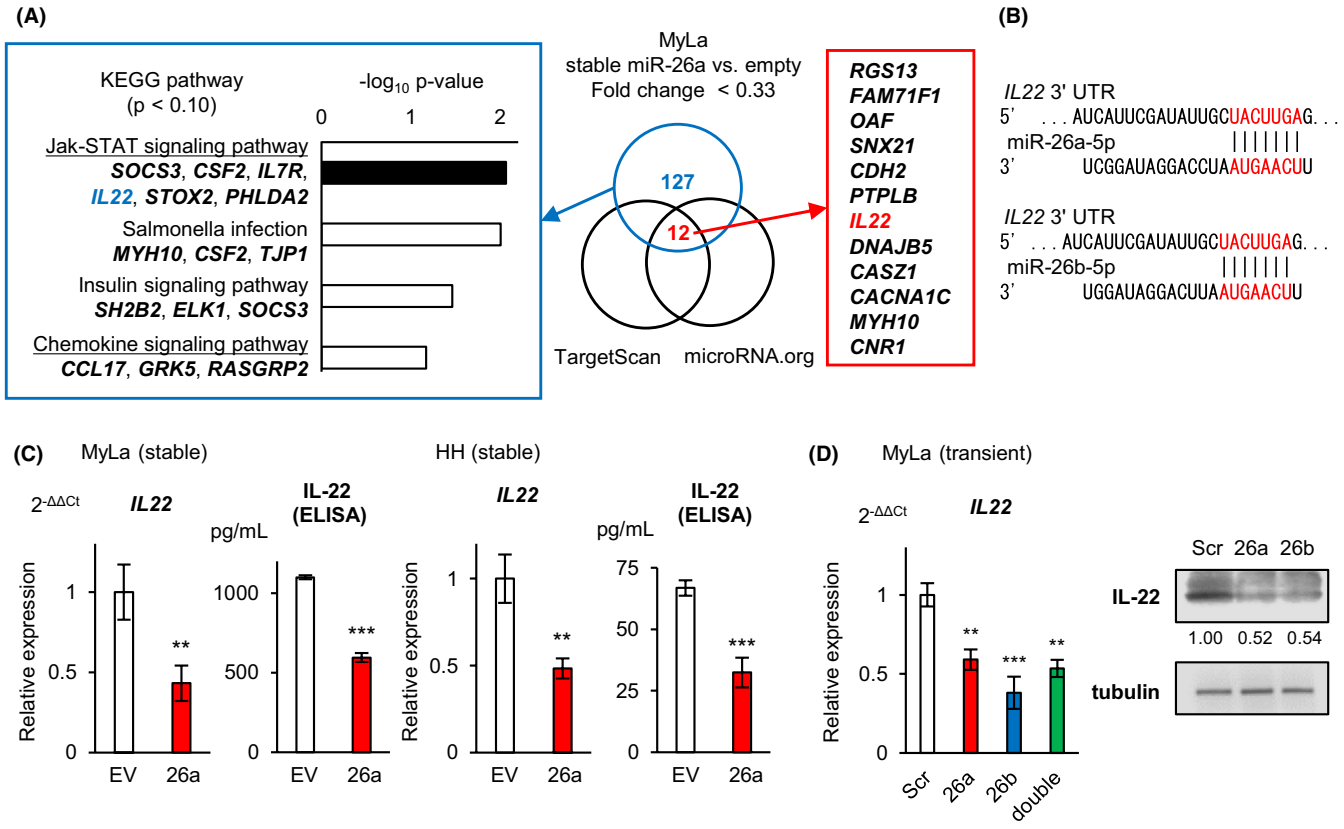

FIGURE 3 IL-22 is the most likely candidate target of miR-26 in CTCL. (A) Detection of potential miR-26a target genes in MyLa. (Left): KEGG analysis of 127 downregulated genes in MyLa transduced with GFP-miR-26a lentivirus vector, compared with GFP-empty lentivirus vector. (Right): List of miR-26 targets of these 127 genes predicted using the indicated two programs *in silico*. (B) Sequence alignment of the mature miR-26a/26b seed sequence and the 3′ untranslated region (UTR) of *IL22*. (C) RT-qPCR analysis of *IL22* and ELISA analysis of IL-22 in MyLa and HH transduced with GFP-empty (control) lentivirus vector or GFP-miR-26a lentivirus vector. EV, empty vector. (D) RT-qPCR analysis of *IL22* in MyLa transiently transduced with scramble control (Scr), miR-26a, miR-26b, or miR-26a+miR-26b (shown as "double") for 24 h. (Right): Western blot analysis of IL-22 in MyLa transiently transduced with Scr, miR-26a, or miR-26b for 48 h. Fold changes in IL-22 levels are shown below the bands. Asterisks indicate statistical significance: *$0.01 \le p < 0.05$; **$0.001 \le p < 0.01$; ***$p < 0.001$; NS, not significant. Student *t*-test was used to test for significance. Bars represent the mean ± 95% confidence intervals of the three replicates

TABLE 1 List of genes whose expression was reduced to one-third or less after stable transduction with miR-26a into MyLa compared with the control, and predicted to bind by the two prediction programs

Gene symbol	Fold change	Description
RGS13	0.13	*Homo sapiens* regulator of G-protein signaling 13 (RGS13), transcript variant 1, mRNA [NM_002927]
FAM71F1	0.19	*Homo sapiens* family with sequence similarity 71, member F1 (FAM71F1), transcript variant 1, mRNA [NM_032599]
OAF	0.20	*Homo sapiens* OAF homolog (*Drosophila*) (OAF), mRNA [NM_178507]
SNX21	0.23	*Homo sapiens* sorting nexin family member 21 (SNX21), transcript variant 4, mRNA [NM_001042633]
CDH2	0.24	*Homo sapiens* cadherin 2, type 1, N-cadherin (neuronal) (CDH2), mRNA [NM_001792]
PTPLB	0.24	*Homo sapiens* protein tyrosine phosphatase-like (proline instead of catalytic arginine), member b (PTPLB), mRNA [NM_198402]
IL22	0.27	*Homo sapiens* interleukin 22 (IL22), mRNA [NM_020525]
DNAJB5	0.27	*Homo sapiens* DnaJ (Hsp40) homolog, subfamily B, member 5 (DNAJB5), transcript variant 3, mRNA [NM_012266]
CASZ1	0.30	*Homo sapiens* castor zinc finger 1 (CASZ1), transcript variant 1, mRNA [NM_001079843]
CACNA1C	0.31	*Homo sapiens* calcium channel, voltage-dependent, L type, alpha 1C subunit (CACNA1C), transcript variant 1, mRNA [NM_199460]
MYH10	0.32	*Homo sapiens* myosin, heavy chain 10, non-muscle (MYH10), transcript variant 1, mRNA [NM_001256012]
CNR1	0.33	*Homo sapiens* cannabinoid receptor 1 (brain) (CNR1), transcript variant 2, mRNA [NM_033181]

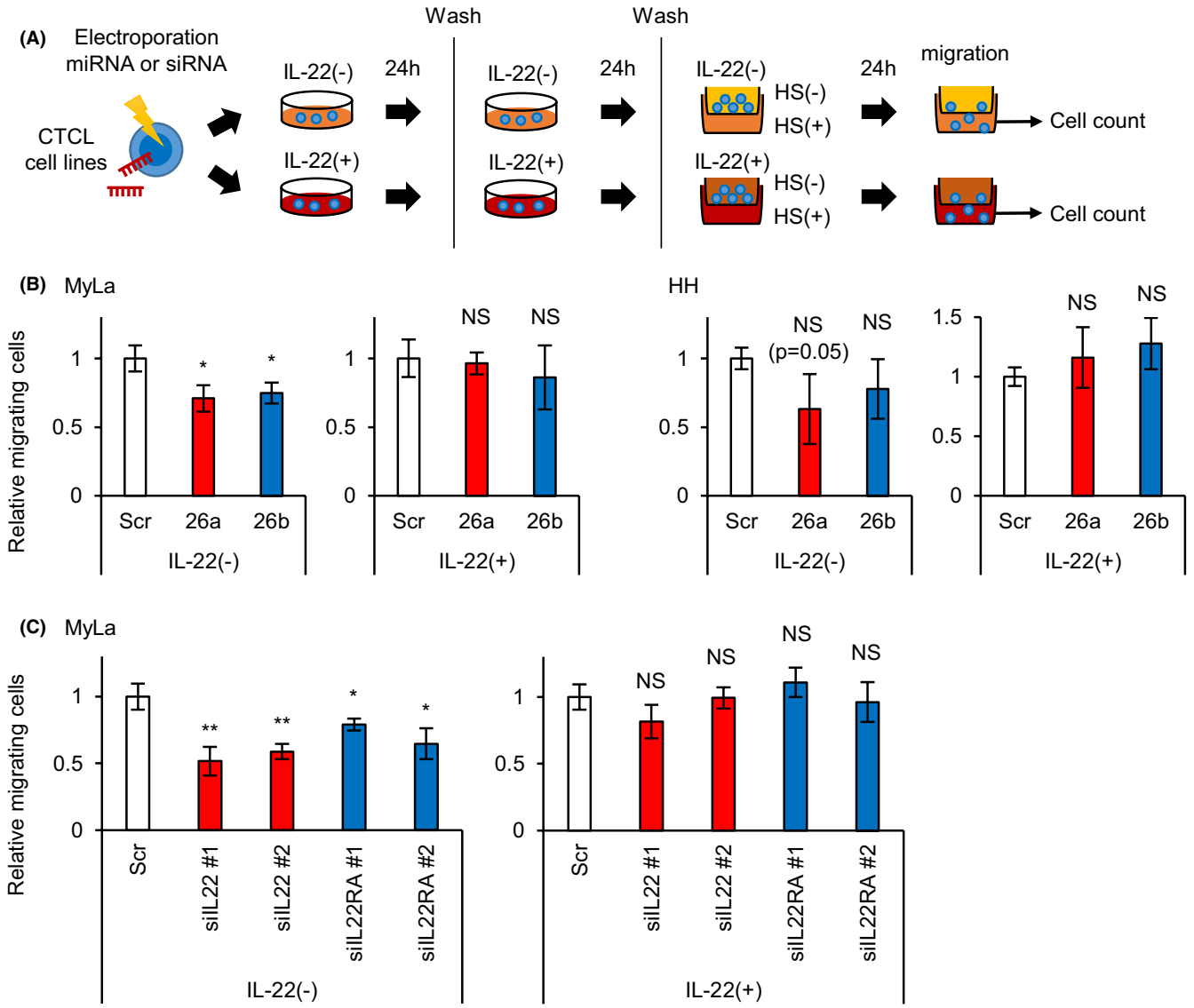

FIGURE 4 miR-26–IL-22–IL22R axis regulates cell migration in CTCL. (A) An experimental design of the migration assay in CTCL cell lines. HS, human serum. (B) Migration assay of MyLa or HH transiently transduced with scramble miRNA (Scr) or miR-26a or 26b and treated with or without IL-22 (50 ng/mL). (C) Migration assay of MyLa transiently transduced with scramble siRNA, siIL22 (two sequences designated as #1 and #2) or siIL22RA (two sequences designated as #1 and #2) and treated with or without IL-22 (50 ng/mL). Asterisks indicate statistical significance: *$0.01 \le p < 0.05$; **$0.001 \le p < 0.01$; *** $p < 0.001$; NS, not significant. Student *t*-test was used to test for significance. Bars represent the mean ± 95% confidence interval of the three replicates

ELISA demonstrated that the addition of shIL22 #D significantly reduced IL-22 production by ~50% compared with the control (Figure 5B). Western blot analysis demonstrated an apparent reduction in IL-22 levels in both shIL22 #C and shIL22 #D transfectants (Figure 5C). These results demonstrated that shIL22 #D suppressed IL-22 production. We used shIL22 #D-transduced MyLa for subsequent *in vitro* and *in vivo* experiments. In the cell proliferation assay, we observed a trend of fewer viable cells with shIL22-transfected cells at 72 h and a significant decrease in viable cells at 96 h compared with the control (Figure 5D). Cell cycle assays exhibited an increase in the subG1 fraction, but not cell cycle arrest (Figure 5E), suggesting that IL22 knockdown induced apoptosis in MyLa cells. The migration assay showed a significant reduction in the migration capability of shIL22-transfected cells (Figure 5F). These results indicated that decreased IL-22 led to impaired cell migration and enhanced apoptosis. Finally, we subcutaneously injected NOG mice with GFP-transfected or GFP-shIL22-transfected MyLa (1×10^6 cells per mouse) and evaluated the effect of shIL22 on tumorigenesis *in vivo*. On day 42, an individual mouse in the control group died because of what we considered to be multiorgan failure resulting from systemic metastasis; therefore, we sacrificed all mice on the same day. Consequently, visible splenomegaly and hepatomegaly were observed in all control groups, but not at all in the shIL22 group (Figure 5G). Hematoxylin and eosin staining showed diffuse tumor infiltration in many organs in the control group, whereas only rare focal tumor infiltration of the spleen was observed in the shIL22 group (Figure S3). These results

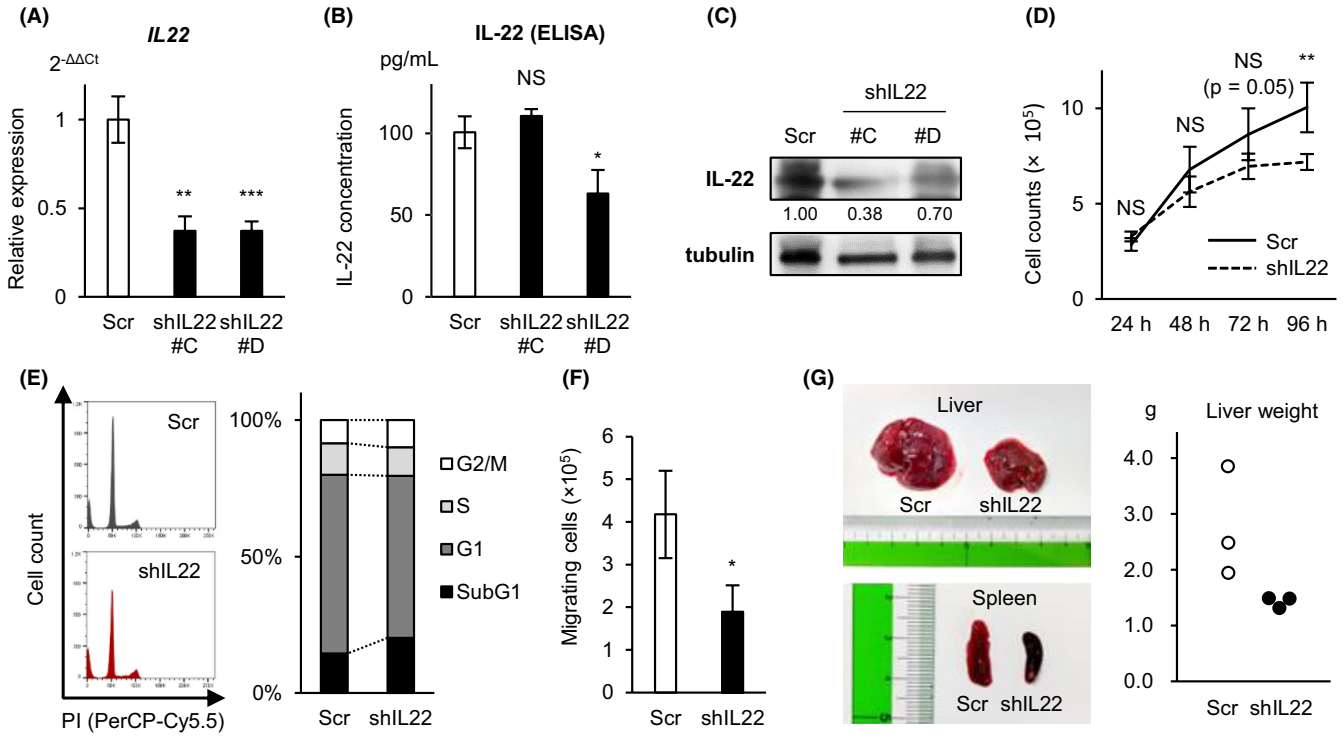

FIGURE 5 IL22 knockdown inhibits invasion and metastasis of CTCL cells *in vivo*. (A) RT-qPCR analysis of *IL22* in MyLa transduced with GFP-scramble (Scr) or GFP-shIL22 (#C, #D) lentivirus vector. (B) ELISA analysis of IL-22 in MyLa transduced with GFP-scramble (Scr) or GFP-shIL22 (#C, #D) lentivirus vector. (C) Western blot analysis of IL-22 in MyLa transduced with GFP-scramble (Scr) or GFP-shIL22 (#C, #D) lentivirus vector. (D) Proliferation assay of MyLa transduced with GFP-scramble (Scr) or GFP-shIL22 #D lentivirus vector. (E) Cell cycle analysis of MyLa transduced with GFP-scramble (Scr) or GFP-shIL22 #D lentivirus vector. (Left): Flow cytometry analysis with propidium iodide (PI) staining is shown. X-axis: PI staining; Y-axis: cell counts. (Right): DNA content (%) of subG1 ($N < 2n$), G1 ($N = 2n$), S ($2n < N < 4n$) and G2/M ($N = 4n$) phases are shown. (F) Migration assay of MyLa transduced with GFP-scramble or GFP-shIL22 #D lentivirus vector cultured for 24 h. (G) (Left): Photographs show the liver and spleen from NOG mouse after transplantation of MyLa transduced with GFP-scramble or GFP-shIL22 #D lentivirus vector (day 42). (Right): Liver weights of the two groups are shown. Asterisks indicate statistical significance: *$0.01 \le p < 0.05$; **$0.001 \le p < 0.01$; ***$p < 0.001$; NS, not significant. Student *t*-test was used to test for significance. Bars represent the mean ± 95% confidence interval of the three replicates

strongly suggested that IL-22 contributes to the malignant development of CTCL by promoting cell survival and organ invasion.

4 | DISCUSSION

Several groups, including ours, have reported comprehensive research for miRNA specifically expressed in CTCL, and for miRNA whose expression changes during disease progression.[15,18,29,30] For example, in advanced but not early CTCL, HDAC and/or MYC activation induced the repression of a tumor-suppressive microRNA, miR-150, whose downregulation contributes to the acquisition of invasion and metastasis.[18] miR-26 is included in the group of the tumor-suppressive miRNAs whose expression is suppressed as CTCL progresses.[31] miR-26 was first reported in 2006 as one of several candidate tumor-suppressive miRNA that are downregulated by a transcription factor, MYC.[24] Actually, miR-26 expression is suppressed in many solid tumors, such as hepatocellular carcinoma and some gastrointestinal cancers.[26] Especially in hepatocellular carcinoma, appropriate delivery systems for miR-26 were able to be used of direct therapy against tumor cells.[32] In hematopoietic malignancies such as acute myelogenous leukemia and multiple myeloma, miR-26 expression is suppressed, and shown to act as a tumor-suppressive miRNA by repressing EZH2 and CD38.[33,34] Notably, even in a same cancer subtype, a certain miRNA may have distinct targets based on disease progression with distinct gene expression profiles.[35] In this study, we showed that *IL22* is the miR-26 target and is involved in invasion and metastasis in advanced CTCL (Figure 6A); however, the function and target molecules of miR-26 in early-stage CTCL remains unknown. Therefore, there is a need to investigate whether miR-26 may represent a distinct expression pattern in different CTCL stages.

We have previously demonstrated the following points regarding mechanisms of invasion and metastasis in advanced CTCL:

(1) miR-150 inhibits invasion and metastasis by targeting the chemokine receptor CCR6.[18]

(2) STAT3 activation caused by the IL-22 autocrine mechanism enhances the transcription of CCL20, a ligand of CCR6, leading to invasion and metastasis.[20]

(3) HDAC inhibitors restore some tumor-suppressive miRNA.[21]

Notably, HDAC inhibitors restored miR-150 and miR-26, and these miRNA revealed an exceedingly similar expression pattern

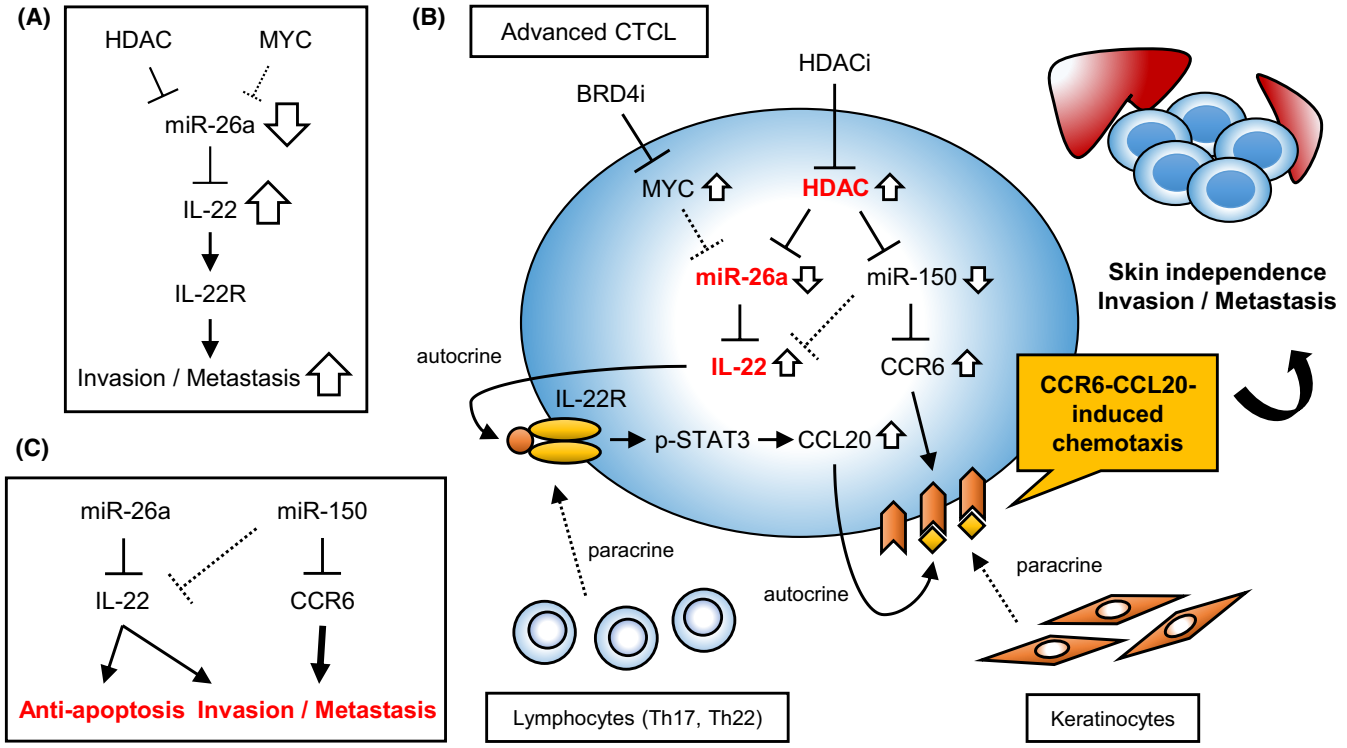

FIGURE 6 miRNA and IL-22 dysregulations involved in invasion and metastasis of advanced CTCL. (A) miR-26a-IL22 axis involved in CTCL invasion and metastasis from the present study. (B) Schema of miRNA dysregulations involved in CTCL invasion and metastasis from our present and previous studies. (C) Two miRNA dysregulations with anti-apoptosis ability and involved in invasion/metastasis in CTCL

(Figure 1). Taken together, these results strongly suggested that downregulation of these miRNA could corroborate the induction of the IL-22–STAT3–CCL20–CCR6 cascade, leading to invasion and metastasis of CTCL (Figure 6B). These results also suggested the efficacy of HDAC inhibitors in advanced CTCL. Importantly, IL-22 suppression caused by miR-26 also induced apoptosis (Figure 6C). Of note, as the ability to induce apoptosis was not observed in miR-150,[18] the miR-26-IL22 cascade may have additional tumor-suppressive capabilities other than that of miR-150. Our results showed that there was an increase in cell death with the transduction of shIL22, but not miR-26. The reason for this is that miR-26 may have a variety of targets other than *IL22*, as shown in Figure 3A and Table 1. Therefore, suppression of other targets may be involved in the attenuation of the pro-apoptotic effect. As we will discuss later, we suggest that direct inhibition of IL-22 may be beneficial.

In the present study, JQ1 did not restore miR-26 expression, whereas HDAC inhibitors restored miRNA expression (Figure 1), suggesting that HDAC inhibitors are more effective than JQ1 in advanced CTCL treatment. However, the efficacy of HDAC inhibitors depends on their ability to activate tumor-suppressive miRNA or tumor-suppressive proteins, such as p53, whose transcription could be activated by its acetylation.[36,37] However, when genomic structural aberrations occur in target tumor-suppressive genes during tumor development, there appears to be a lower expectation for epigenetic restoration effect of the target tumor-suppressive genes.[37-39] In these cases, antibody therapy may be available. Indeed, along with surface antigens such as CD30 and CCR4, the humoral factor IL-22 is a candidate for novel therapeutic antibody targets. IL-22 is a cytokine from the IL-10 family that is produced by activated T cells, particularly T helper (Th)22 and Th17.[40] IL-22 acts through Jak–STAT pathway activation to maintain and proliferate epidermal keratinocytes, airway epithelial cells, synovial fibroblasts, intestinal epithelial cells, hepatocytes, and pancreatic cells when its cascade is adequately regulated. However, if it is not appropriately regulated, the onset of a variety of diseases may be increased, including inflammatory skin diseases, inflammatory bowel disease, graft-versus-host disease, and cancers including solid tumors such as colon cancer and certain malignant lymphomas.[41,42] As IL-22 mRNA and protein are highly expressed in the serum and lesions of CTCL patients,[27,28] the development of IL-22 neutralizing antibodies may be promising for CTCL treatment. Neutralizing antibodies to interleukins are currently in clinical use for several diseases. Mepolizumab (anti-IL-5 antibody) is used for allergic diseases such as asthma and eosinophilic polyangiitis granulomatosa.[43] Secukinumab (anti-IL-17A antibody) and risankizumab (anti-IL-23 antibody) are clinically used for certain collagen diseases and psoriasis.[44,45] In skin diseases, such as psoriasis, immunocompetent cell suppression by interleukin neutralizing antibodies is useful, and this suggests that a similar treatment mechanism may be advantageous in CTCL. In CTCL, inflammatory molecules released from the tumor itself and/or surrounding immune cells are known to play a crucial role in tumor migration into multiple organs.[18,27] Therefore, it is worthwhile to experimentally evaluate the therapeutic effects of conventional chemotherapy versus HDAC inhibitor with IL-22 neutralizing antibody in the near future.

In summary, our study strongly suggests that the miR-26–IL-22 axis is deeply involved in the molecular pathogenesis of advanced CTCL and provides a scientific basis for IL-22-targeted therapy. Therapies targeting fluid factors are expected to be developed to avoid progression to advanced CTCL.

ACKNOWLEDGMENTS

The authors would like to thank Yukiko Abe, Yuko Chiba, and Hiromi Kataho for their outstanding technical assistance.

DISCLOSURE

NT received honoraria from Pfizer, Otsuka, and Novartis, and research funding from Novartis. AK received honoraria from Janssen.

ORCID

Sho Ikeda https://orcid.org/0000-0002-3780-2993
Akihiro Kitadate https://orcid.org/0000-0003-3218-2446
Naoto Takahashi https://orcid.org/0000-0002-6758-3787

REFERENCES

1. Armitage JO, Gascoyne RD, Lunning MA, Cavalli F. Non-Hodgkin lymphoma. *Lancet*. 2017;390:298-310.
2. Vaqué JP, Martínez N, Batlle-López A, et al. B-cell lymphoma mutations: improving diagnostics and enabling targeted therapies. *Haematologica*. 2014;99:222-231.
3. Ennishi D, Jiang A, Boyle M, et al. Double-hit gene expression signature defines a distinct subgroup of germinal center B-cell-like diffuse large B-cell lymphoma. *J Clin Oncol*. 2019;37:190-201.
4. Susanibar-Adaniya S, Barta SK. 2021 Update on Diffuse large B cell lymphoma: A review of current data and potential applications on risk stratification and management. *Am J Hematol*. 2021;96:617-629.
5. Rosenquist R, Beà S, Du MQ, Nadel B, Pan-Hammarström Q. Genetic landscape and deregulated pathways in B-cell lymphoid malignancies. *J Intern Med*. 2017;282:371-394.
6. Morin RD, Arthur SE, Assouline S. Treating lymphoma is now a bit EZ-er. *Blood Adv*. 2021;5:2256-2263.
7. Broccoli A, Zinzani PL. Peripheral T-cell lymphoma, not otherwise specified. *Blood*. 2017;129:1103-1112.
8. Wang H, Fu BB, Gale RP, Liang Y. NK-/T-cell lymphomas. *Leukemia*. 2021;35:2460-2468.
9. Ikeda S, Tagawa H. Dysregulation of microRNAs and their association in the pathogenesis of T-cell lymphoma/leukemias. *Int J Hematol*. 2014;99:542-552.
10. Ahmed N, Feldman AL. Targeting epigenetic regulators in the treatment of T-cell lymphoma. *Expert Rev Hematol*. 2020;13:127-139.
11. Hristov AC, Tejasvi T, Wilcox RA. Mycosis fungoides and Sézary syndrome: 2019 update on diagnosis, risk-stratification, and management. *Am J Hematol*. 2019;94:1027-1041.
12. Scarisbrick JJ, Bagot M, Ortiz-Romero PL. The changing therapeutic landscape, burden of disease, and unmet needs in patients with cutaneous T-cell lymphoma. *Br J Haematol*. 2021;192:683-696.
13. Photiou L, van der Weyden C, McCormack C, Miles PH. Systemic treatment options for advanced-stage mycosis fungoides and sézary syndrome. *Curr Oncol Rep*. 2018;20:32.
14. Kempf W, Mitteldorf C. Cutaneous T-cell lymphomas-An update 2021. *Hematol Oncol*. 2021;39(Suppl 1):46-51.
15. Sandoval J, Díaz-Lagares A, Salgado R, et al. MicroRNA expression profiling and DNA methylation signature for deregulated microRNA in cutaneous T-cell lymphoma. *J Invest Dermatol*. 2015;135:1128-1137.
16. Bartel DP. Metazoan MicroRNAs. *Cell*. 2018;173(1):20-51.
17. Lee YS, Dutta A. MicroRNAs in cancer. *Annu Rev Pathol*. 2009;4:199-227.
18. Ito M, Teshima K, Ikeda S, et al. MicroRNA-150 inhibits tumor invasion and metastasis by targeting the chemokine receptor CCR6, in advanced cutaneous T-cell lymphoma. *Blood*. 2014;123:1499-1511.
19. Kitadate A, Ikeda S, Teshima K, et al. MicroRNA-16 mediates the regulation of a senescence-apoptosis switch in cutaneous T-cell and other non-Hodgkin lymphomas. *Oncogene*. 2016;35:3692-3704.
20. Ikeda S, Kitadate A, Ito M, et al. Disruption of CCL20-CCR6 interaction inhibits metastasis of advanced cutaneous T-cell lymphoma. *Oncotarget*. 2016;7:13563-13574.
21. Abe F, Kitadate A, Ikeda S, et al. Histone deacetylase inhibitors inhibit metastasis by restoring a tumor suppressive microRNA-150 in advanced cutaneous T-cell lymphoma. *Oncotarget*. 2017;8:7572-7585.
22. Tagawa H, Ikeda S, Sawada K. Role of microRNA in the pathogenesis of malignant lymphoma. *Cancer Sci*. 2013;104:801-809.
23. Kohnken R, Wen J, Mundy-Bosse B, et al. Diminished microRNA-29b level is associated with BRD4-mediated activation of oncogenes in cutaneous T-cell lymphoma. *Blood*. 2018;131:771-781.
24. Chang TC, Yu D, Lee YS, et al. Widespread microRNA repression by Myc contributes to tumorigenesis. *Nat Genet*. 2008;40:43-50.
25. Kanavaros P, Ioannidou D, Tzardi M, et al. Mycosis fungoides: expression of C-myc p62 p53, bcl-2 and PCNA proteins and absence of association with Epstein-Barr virus. *Pathol Res Pract*. 1994;190:767-774.
26. Li C, Li Y, Lu Y, et al. miR-26 family and its target genes in tumorigenesis and development. *Crit Rev Oncol Hematol*. 2020;157:103124.
27. Miyagaki T, Sugaya M, Suga H, et al. IL-22, but not IL-17, dominant environment in cutaneous T-cell lymphoma. *Clin Cancer Res*. 2011;17:7529-7538.
28. Papathemeli D, Patsatsi A, Papanastassiou D, et al. Protein and mRNA expression levels of interleukin-17A, -17F and -22 in blood and skin samples of patients with mycosis fungoides. *Acta Derm Venereol*. 2020;100(18):adv00326.
29. Ralfkiaer U, Hagedorn PH, Bangsgaard N, et al. Diagnostic microRNA profiling in cutaneous T-cell lymphoma (CTCL). *Blood*. 2011;118:5891-5900.
30. Shen X, Wang B, Li K, et al. MicroRNA signatures in diagnosis and prognosis of cutaneous T-Cell lymphoma. *J Invest Dermatol*. 2018;138:2024-2032.
31. Manso R, Martínez-Magunacelaya N, Eraña-Tomás I, et al. Mycosis fungoides progression could be regulated by microRNAs. *PLoS One*. 2018;13:e0198477.
32. Kota J, Chivukula RR, O'Donnell KA, et al. Therapeutic microRNA delivery suppresses tumorigenesis in a murine liver cancer model. *Cell*. 2009;137:1005-1017.
33. Salvatori B, Iosue I, Djodji Damas N, et al. Critical role of c-Myc in acute myeloid leukemia involving direct regulation of miR-26a and histone methyltransferase EZH2. *Genes Cancer*. 2011;2:585-592.
34. Hu Y, Liu H, Fang C, et al. Targeting of CD38 by the tumor suppressor miR-26a serves as a novel potential therapeutic agent in multiple myeloma. *Cancer Res*. 2020;80:2031-2044.
35. Verma S, Pandey M, Shukla GC, Singh V, Gupta S. Integrated analysis of miRNA landscape and cellular networking pathways in stage-specific prostate cancer. *PLoS One*. 2019;14:e0224071.
36. Newbold A, Falkenberg KJ, Prince HM, Johnstone RW. How do tumor cells respond to HDAC inhibition? *FEBS J*. 2016;283:4032-4046.
37. Yu X, Li H, Zhu M, et al. Involvement of p53 acetylation in growth suppression of cutaneous T-cell lymphomas induced by HDAC inhibition. *J Invest Dermatol*. 2020;140:2009-2022.e4.
38. Loganzo F, Sung M, Gerber HP. Mechanisms of resistance to antibody-drug conjugates. *Mol Cancer Ther*. 2016;15:2825-2834.

39. da Silva Almeida AC, Abate F, Khiabanian H, et al. The mutational landscape of cutaneous T cell lymphoma and Sézary syndrome. *Nat Genet*. 2015;47:1465-1470.
40. Pestka S, Krause CD, Sarkar D, Walter MR, Shi Y, Fisher PB. Interleukin-10 and related cytokines and receptors. *Annu Rev Immunol*. 2004;22:929-979.
41. Sabat R, Ouyang W, Wolk K. Therapeutic opportunities of the IL-22-IL-22R1 system. *Nat Rev Drug Discov*. 2014;13:21-38.
42. Hernandez P, Gronke K, Diefenbach A. A catch-22: Interleukin-22 and cancer. *Eur J Immunol*. 2018;48:15-31.
43. Haldar P, Brightling CE, Hargadon B, et al. Mepolizumab and exacerbations of refractory eosinophilic asthma. *N Engl J Med*. 2009;360:973-984.
44. McInnes IB, Mease PJ, Kirkham B, et al. Secukinumab, a human anti-interleukin-17A monoclonal antibody, in patients with psoriatic arthritis (FUTURE 2): a randomised, double-blind, placebo-controlled, phase 3 trial. *Lancet*. 2015;386:1137-1146.
45. Gordon KB, Strober B, Lebwohl M, et al. Efficacy and safety of risankizumab in moderate-to-severe plaque psoriasis (UltIMMa-1 and UltIMMa-2): results from two double-blind, randomised, placebo-controlled and ustekinumab-controlled phase 3 trials. *Lancet*. 2018;392:650-661.

SUPPORTING INFORMATION

Additional supporting information may be found in the online version of the article at the publisher's website.

How to cite this article: Matsuda Y, Ikeda S, Abe F, et al. Downregulation of miR-26 promotes invasion and metastasis via targeting interleukin-22 in cutaneous T-cell lymphoma. *Cancer Sci*. 2022;113:1208–1219. doi:10.1111/cas.15296